Journal of Visualized Experiments

Using a Cyclic Ion Mobility Spectrometer for Tandem Ion Mobility Experiments

--Manuscript Draft--

Article Type:	Invited Methods Collection - JoVE Produced Video
Manuscript Number:	JoVE63451R2
Full Title:	Using a Cyclic Ion Mobility Spectrometer for Tandem Ion Mobility Experiments
Corresponding Author:	Helene Rogniaux, Ph.D. INRAE: Institut National de Recherche pour l'Agriculture l'Alimentation et l'Environnement NANTES, Pays-de-la-Loire FRANCE
Corresponding Author's Institution:	INRAE: Institut National de Recherche pour l'Agriculture l'Alimentation et l'Environnement
Corresponding Author E-Mail:	helene.rogniaux@inrae.fr
Order of Authors:	Simon Ollivier
	Mathieu Fanuel
	Helene Rogniaux, Ph.D.
	David Ropartz
Additional Information:	
Question	**Response**
Please specify the section of the submitted manuscript.	Chemistry
Please indicate whether this article will be Standard Access or Open Access.	Standard Access ($1400)
Please indicate the **city, state/province, and country** where this article will be **filmed**. Please do not use abbreviations.	Nantes, Pays-de-la-Loire, FRANCE
Please confirm that you have read and agree to the terms and conditions of the author license agreement that applies below:	I agree to the Author License Agreement
Please confirm that you have read and agree to the terms and conditions of the video release that applies below:	I agree to the Video Release
Please provide any comments to the journal here.	

TITLE:

Using a Cyclic Ion Mobility Spectrometer for Tandem Ion Mobility Experiments

AUTHORS AND AFFILIATIONS:

Simon Ollivier[1,2], Mathieu Fanuel[1,2], Hélène Rogniaux[1,2], David Ropartz[1,2]

[1]INRAE, UR BIA, F-44316 Nantes, France
[2]INRAE, BIBS Facility, F-44316 Nantes, France

Email addresses of co-authors:

Simon Ollivier	(simon.ollivier@inrae.fr)
Mathieu Fanuel	(mathieu.fanuel@inrae.fr)
David Ropartz	(david.ropartz@inrae.fr)

Corresponding author:

Hélène Rogniaux	helene.rogniaux@inrae.fr

SUMMARY:

Ion mobility spectrometry (IMS) is an interesting complement to mass spectrometry for the characterization of biomolecules, notably because it is sensitive to isomerism. This protocol describes a tandem IMS (IMS/IMS) experiment, which allows the isolation of a molecule and the generation of the mobility profiles of its fragments.

ABSTRACT:

Accurate characterization of chemical structures is important to understand their underlying biological mechanisms and functional properties. Mass spectrometry (MS) is a popular tool but is not always sufficient to completely unveil all structural features. For example, although carbohydrates are biologically relevant, their characterization is complicated by numerous levels of isomerism. Ion mobility spectrometry (IMS) is an interesting complement because it is sensitive to ion conformations and, thus, to isomerism.

Furthermore, recent advances have significantly improved the technique: the last generation of Cyclic IMS instruments offers additional capabilities compared to linear IMS instruments, such as an increased resolving power or the possibility to perform tandem ion mobility (IMS/IMS) experiments. During IMS/IMS, an ion is selected based on its ion mobility, fragmented, and reanalyzed to obtain ion mobility information about its fragments. Recent work showed that the mobility profiles of the fragments contained in such IMS/IMS data can act as a fingerprint of a particular glycan and can be used in a molecular networking strategy to organize glycomics datasets in a structurally relevant way.

The goal of this protocol is thus to describe how to generate IMS/IMS data, from sample preparation to the final Collision Cross Section (CCS) calibration of the ion mobility dimension that yields reproducible spectra. Taking the example of one representative glycan, this protocol will show how to build an IMS/IMS control sequence on a Cyclic IMS instrument, how to account

for this control sequence to translate IMS arrival time into drift time (i.e., the effective separation time applied to the ions), and how to extract the relevant mobility information from the raw data. This protocol is designed to clearly explain the critical points of an IMS/IMS experiment and thus help new Cyclic IMS users perform straightforward and reproducible acquisitions.

INTRODUCTION:

The complete chemical characterization of biomolecules is key to understanding their underlying biological and functional properties. To this end, "omics" sciences have developed in recent years, aiming for the large-scale characterization of chemical structures at biological concentrations. In proteomics and metabolomics, MS has become a core tool to unravel the structural heterogeneity found in biological media—notably thanks to its sensitivity and ability to provide structural information through tandem MS (MS/MS). In MS/MS strategies, an ion is selected according to its mass, then fragmented, and finally, the masses of its fragments are acquired to establish a fingerprint of the molecule. MS/MS spectra can, in particular, be used to match spectral databases[1,2], or tentatively reconstruct the parent structures[3,4]. Under the assumption that similar spectra belong to similar compounds, MS/MS data can also be used to build molecular networks (MNs) connecting related species through a similarity score[5,6].

However, because of the inherent property of MS to detect the mass-to-charge ratio (*m/z*) of ions, the technique is blind to a number of structural features that fall within the range of (stereo)isomerism. For example, carbohydrates are made of several monosaccharide subunits, many of which are stereoisomers or even epimers (e.g., Glc vs. Gal or Glc vs. Man). These subunits are linked by glycosidic bonds, which can differ by the position of the linkage (regioisomerism) and the steric configuration of the anomeric carbon (anomerism). These characteristics make it difficult for standalone MS to distinguish between carbohydrate isomers[7], and only regioisomerism can be addressed using high-energy activation methods[8–10]. Although derivatization is an option to disrupt the equivalence of stereoisomeric groups[11], it requires extensive sample preparation. Another, more straightforward option is to couple MS with an analytical dimension sensitive to isomerism, such as IMS.

Because this protocol is designed for users who are already familiar with the basic concepts of IMS, and because detailed reviews are available elsewhere[12,13], only a brief overview of the principles of IMS is given here. IMS is a gas-phase separation method that relies on the interaction of ions with a buffer gas and an electric field, ultimately separating ions according to their gas-phase conformations. Different principles of IMS coupled to MS can be found on commercial instruments: some operate at alternating high and low electric fields (field asymmetric IMS, FAIMS), while most operate within the low field limit—notably drift tube IMS (DTIMS, linearly decreasing electric field), traveling wave IMS (TWIMS, symmetric potential waves), and trapped IMS (TIMS, high flow of buffer gas trapping ions against electric fields)[13]. The low-field methods allow access to a so-called CCS, a property of the ion–gas pair that represents the surface (in $Å^2$ or nm^2) of the ion that interacts with the buffer gas during the separation. CCS is theoretically instrument-independent and is thus useful to generate data that can be reproduced between different laboratories[14]. Ion mobility separations can be impacted by various parameters and, notably, by fluctuations of the gas pressure and gas temperature in the mobility cell. The CCS

calibration is a way to remedy this, as both the calibrant and the species of interest will be similarly affected[13]. However, it is mandatory to install the instrument in a temperature-controlled room and to have a reliable gas pressure control system.

An interesting evolution of IMS is IMS/IMS, which was first introduced in 2006 by Clemmer's group as an analog of MS/MS[15,16]. In IMS/IMS, an ion of interest is selectively isolated based on its ion mobility; it is then activated (until possible fragmentation), and a new IMS analysis of the activated ion or fragments is performed. In the first instrumental design, two IMS cells were put in series, separated by an ion funnel where the activation stood. Since then, although a number of IMS/IMS setups were proposed (for a review, see Eldrid and Thalassinos[17]), the first commercial mass spectrometer with IMS/IMS capability only became available in 2019[18]. This instrument substantially improved the initial concept by combining it with another technological breakthrough: a cyclic design of the IMS cell.

The cyclic IMS cell theoretically allows increasing near-infinitely the drift path length and, thus, the resolving power of the instrument[19]. This was achieved by means of a particular instrument geometry, where the cyclic TWIMS cell is placed orthogonally to the main ion optical axis. A multifunction array region at the entrance of the IMS cell allows controlling the direction of the ion path: (i) sending ions sideways for IMS separation, (ii) forward for MS detection, or (iii) backward from the IMS cell to be stored in a prearray cell. From this prearray store cell, the ions can be activated and the fragments reinjected in the IMS cell for ion mobility measurement, an approach that has been successfully used to characterize stereoisomers[20]. Ultimately, the collected data contain ion mobility and *m/z* information for the precursor and its fragments.

In a recent publication that used this cyclic design for glycan analyses (Ollivier et al.[21]), we showed that the mobility profile of the fragments contained in such IMS/IMS data acts as a fingerprint of a biomolecule that can be used in a molecular networking strategy. The resulting network, called IM-MN, led to the organization of glycomics datasets in a structurally relevant way, whereas the network built solely from MS/MS data (MS-MN) revealed little information. To complement this publication and help Cyclic IMS users implement this workflow, this protocol provides a complete description of the protocol used to collect the data. This protocol focuses only on the generation of the IMS/IMS data that users can then use to build IM-MN networks (see[21])—or for any other application of their choice. Building of IM-MN will not be considered herein, as protocols for molecular networking are already available[22]. The crucial points that must be followed to generate valuable and reproducible IMS/IMS acquisitions are highlighted. Taking the example of one of the oligosaccharides studied by Ollivier *et al.*[21], the following steps are detailed: (i) sample preparation, (ii) tuning of the Cyclic IMS instrument, (iii) automated peak-picking of the data, and (iv) CCS calibration.

PROTOCOL:

NOTE: An overview of the protocol is provided in **Figure 1**. The parameters used for the experiments described in the present protocol can be found in **Supplemental Table S1** and **Supplemental Table S2**.

1. Preparation of the sample solution

NOTE: The protocol is described using an arabinoxylan pentasaccharide (2^3-α-L-arabinofuranosyl-xylotetraose or XA^2XX; see the **Table of Materials**) as an example.

1.1. Preparation of the solvent: 500 µM LiCl in 50:50 H_2O:MeOH (vol./vol.).

1.1.1. Prepare a 100 mM stock solution of lithium chloride (LiCl) in H_2O by weighing 212 mg of LiCl and add 50 mL of high-purity deionized water (H_2O) in a 50 mL polypropylene conical tube. Shake until completely dissolved.

NOTE: The solvent is doped with a lithium salt to promote the formation of $[M+Li]^+$ adducts in the ion source of the spectrometer, as it usually yields better-quality fragmentation spectra compared to other alkali adducts. The use of LiCl is recommended because organic acids (and thus their salts) have previously been found to impact IMS profiles[23].

1.1.2. In a glass bottle, dilute the LiCl stock solution 200x: to 250 µL of the stock solution, add 24.75 mL of H_2O. Add 25 mL of methanol (MeOH) to reach a final concentration of LiCl of 500 µM in 50:50 H_2O:MeOH (v/v). Sonicate for 2 min to degas the solvent.

NOTE: MeOH presents a health hazard (H225, H301, H311, H331, H370); manipulate under an extractor hood wearing a lab coat, gloves, and eye protection. A proportion of 50:50 MeOH/H_2O (v/v) appears to be the best solvent for the ionization of oligosaccharides; however, MeOH can be substituted by acetonitrile (ACN) if needed.

1.2. In a 1.5 mL polypropylene tube, weigh 1 mg of the carbohydrate. Dissolve with an appropriate volume of 500 µM LiCl to reach a concentration of 1 mg/mL. Dilute to a final concentration of 10 µg/mL in 50:50 MeOH/H_2O + 500 µM LiCl. Store at 4 °C.

NOTE: The concentration of 10 µg/mL was chosen to optimize the signal over all fragment ions during IMS/IMS-MS (this is for a pure compound; increase the concentration when working on mixtures). For the acquisition of reference IMS/IMS spectra, do not dilute the sample further: saturation of the MS detector prior to fragmentation is expected, although the instrument offers options to correct it (see step 3.2.).

2. Tuning of the Cyclic IMS mass spectrometer

NOTE: Software-related instructions (windows, menus, and commands) are highlighted in **bold**.

2.1. Open the instrument console from the instrument control software (**MS tune** page, see the software details in the **Table of Materials**), and put the instrument in **Operate** mode. Wait for at least 3 h for the high voltages to stabilize in the IMS cell.

NOTE: For the best reproducibility, the voltages in the IMS cell need to be completely stabilized. Turn on the high voltages and let the instrument stabilize overnight before any cyclic IMS analysis. Furthermore, the pressure and temperature in the ion mobility cell must be kept as constant as possible. Although a readback for the pressure is available in the **Vacuum** tab, no readback is available for the temperature. Keep the instrument in a thermostated laboratory. The instrument used in this work operates at 1.75 mbar in a laboratory thermostated at 20 °C.

2.2. Cyclic IMS instrument setup

NOTE: Standard solutions must be infused using the built-in fluidics system for the instrument setup.

2.2.1. Place the fluidics containers filled with the appropriate manufacturer-provided standards on the fluidics system: Reservoir B ('Lockmass'): 10 pg/µL leucine enkephaline (LEU ENK) in 50:50 ACN/H_2O + 0.1% formic acid; Reservoir C ('Calibrant'): MajorMix.

NOTE: In this protocol, the MajorMix calibration solution will be used to calibrate both the *m/z* and CCS dimensions. For practical reasons, an external CCS calibration will be performed (see step 5 of the protocol); hence, it is also possible to use an in-house calibrant mixture for the CCS and another calibrant for the *m/z* (e.g., sodium formate or sodium iodide).

2.2.2. On the **Tune** page of the Quartz console, go to the **Fluidics** tab. Set the sample fluidics to reservoir C and the reference fluidics to reservoir B. Infuse both solutions consecutively in the ion source to check the MS signal.

2.2.3. Perform the ADC setup, detector setup (using LEU ENK), and mass calibration (see the **Table of Materials** for the calibration solution) from the **Instrument Setup** page according to the manufacturer's instructions.

2.3. Record an IMS acquisition of the calibration solution with a single pass separation (use this for external IMS calibration).

NOTE: The ion source and the traveling wave (TW) parameters (static wave height and wave velocity) must be kept constant during all the acquisitions (calibration and acquisitions). If the user does not have prior knowledge of the optimal parameters for his sample, this step can be performed after step 3 of the protocol (for $[M+Li]^+$ adducts of neutral oligosaccharides, the representative results use a TW height of 16 V and TW velocity of 350 m/s, which give the best results).

2.3.1. From the **Fluidics** tab, select baffle position **Sample** and infuse the calibrant (see the **Table of Materials**) in the ion source (using the built-in fluidics system) through the 'Sample' probe at a flow rate of 10 µL/min.

2.3.2. Set up a single-pass IMS sequence. From the **Tune** page, put the instrument in **Mobility**

mode, and open the **Cyclic Sequence Control** window. Select **Advanced** mode. From the **Cyclic Functions** tab of this new window, select **Add Bundle**, then **Single/Multipass**. Wait for a sequence of mobility events to appear in the **Sequence** tab of the same window.

NOTE: To activate the real-time display, the user must apply the instrument parameters: click on **Tune** in **TOF** mode or **Run** in **Mobility** mode. Before switching the instrument between **TOF** and **Mobility** modes, it is necessary to **Abort** any running acquisition (including the **Tune** page display). The relative abundance of ions may vary between **TOF** mode and **Mobility** mode because of changes in the ion transmission parameters.

2.3.3. Adapt the sequence so that all the calibrant ions make a single pass around the cyclic IMS racetrack. Do not change the **Inject** time or the **Eject and acquire** time; however, lower the **Separate** time to 1 ms (in the **Sequence** tab). If some ions of the calibration mixture do not fit in the displayed arrival time window, change the synchronization of the IMS with the pusher of the orthogonal acceleration TOF analyzer by increasing the number of **Pushes Per Bin** in the **ADC Settings** tab.

NOTE: The times in the control sequence only control the multifunction array for ion gating. As long as the ions are engaged in their first (or n^{th}) pass around the racetrack, they will finish said pass even if the direction of the TW has changed in the array in the meantime. Lowering the separation time to 1 ms means that the array will switch to ejection mode after 1 ms. This ensures that the faster ions will not have enough time to pass through the array and engage in a second pass before the slower ions finish their first pass. Therefore, all ions will be subjected to the same number of passes (i.e., one pass), which is necessary to perform IMS calibration.

2.3.4. Record a 2-min acquisition. In the **Cyclic Sequence Control** window, click on **Acquire** to open the **Acquisition Settings** popup window. Input the **Filename**, **Description**, and **Length of Acquisition (mins)** and click **Save**.

2.4. Record another 2 min acquisition of the calibration solution under the same conditions as step 2.3 (use this to check the quality of the CCS calibration). In the **Cyclic Sequence Control** window, click on **Acquire** to open the **Acquisition Settings** popup window. Input the **Filename**, **Description**, and **Length of Acquisition (mins)** and click **Save**.

2.5. Thoroughly wash the fluidics system with 50:50 H_2O/ACN to avoid crystallization of the calibrant in the peek tubing.

3. IMS/IMS-MS acquisition

3.1. Using a syringe pump, infuse the (lithium-doped) sample at 10 µg/mL through the sample probe at a flow rate of 10 µL/min.

3.2. Switch the instrument to **TOF** mode (from the **MS tune** page) to check the stability of the signal. Record a full MS acquisition (1 min) of the sample, which will be useful to check the

isotopic pattern and the presence of potential contaminants.

NOTE: Because the sample concentration is chosen to obtain a good ion signal for the fragments, a TOF saturation may be observed at this step. TOF saturation can be identified using the following artifacts: (i) an artificially increased MS resolution, (ii) a change in isotopic ratios, and (iii) a multitude of low-abundance peaks in-between isotopes. Use the **DRE Lens** (Dynamic Range enhancement, **Quad/MS Profile/DRE** tab of the main **Tune** page) to attenuate the transmission of ions and discard the saturation in **TOF** mode (**Figure 2A,B**).

3.3. Put the instrument in **MSMS** mode (**Quad/MS Profile** tab of the main **Tune** page) and select the mass of the targeted ion in the **MSMS Mass** field for isolation in the quadrupole (in the example: *m/z* of 685.2, corresponding to the $[M+Li]^+$ ionic species of the arabinoxylan pentasaccharide). Record a 1 min acquisition to check the precursor isolation when processing the data.

NOTE: Lithium adducts have an isotope at –1 Da of the monoisotopic peak, which needs to be removed from the MS/MS selection window so that it will not interfere with the processing steps. It can be removed by narrowing the selection range using the **LM Resolution** and **HM Resolution** parameters in the **Quad/MS Profile** tab (**Figure 2C**).

3.4. Set up a "slicing" IMS sequence to perform a mobility-based selection of the isomer of interest.

3.4.1. Switch the instrument to **Mobility** mode (see step 2.3.2). In the **Cyclic Sequence Control** window, from the **Cyclic Functions** Tab, select **Add bundle** and then **Slicing**. Wait for a complex sequence of mobility events to appear in the **Sequence** tab (**Figure 3**).

NOTE: It is possible to visualize each step of the IMS/IMS process: click on the **Eject and Acquire** event in the **Sequence** tab. Once highlighted in red, move it to the appropriate position within the sequence using the **Up** and **Down** buttons.

3.4.2. Position the **Eject and Acquire** event right after the first **Separate** event (i.e., move it at row 3 instead of row 8 in the sequence as displayed in **Figure 3**) and then click **Run**. Look for the results of the initial separation to be displayed in real time. Increase the duration of the first **Separate** event for a multipass separation by changing the time value for this event in the sequence until the resolution of the IMS peaks is satisfactory. Record a 1 min acquisition for reference.

NOTE: Take note of the **ADC Start Delay** value in the **ADC Setup** tab: it will be useful to check the quality of the isolation.

3.4.3. Click **Pause**. Note that the results of the initial separation are displayed, although modifications in the control sequence will not be applied until the user clicks **Run** again. Position the **Eject and Acquire** event below the **Eject**, **Eject to Pre-Store**, and **Hold and Eject** events. Adjust

the duration of the events so that the targeted peak is in the **Eject to Pre-Store** region, and any other ion is either in the **Eject** or **Hold and Eject** region.

NOTE: The duration of these three events compared to the arrival time distributions (ATDs) can be visualized using the color-coded bar below the mobility spectrum in the **Mobilogram** tab (**Figure 3**).

3.4.4. Position the **Eject and Acquire** event at the end of the sequence, below the **Reinject from Pre-Store** and the second **Separate** events. Click **Run** to display the selected population.

NOTE: Because the selected population has left the IMS cell, all previous separation has been lost, and it is back to a single-pass separation (which is desired).

3.4.5. Check the quality of the isolation. To verify that only the peak of interest has been selected, perform the same separation after reinjection as before reinjection (i.e., same **Separate** time) as shown in **Figure 4**. Record a 1 min acquisition for reference.

NOTE: The users are encouraged to check the ejected population; the **Eject to Pre-Store** time window should be baseline level (**Figure 4B**). To check this, put the **ADC Start Delay** in **Manual** mode in the **ADC Settings** tab, and enter the delay time noted in step 3.4.2. Record a 1 min acquisition for reference.

3.4.6. In the **Sequence** tab, in the column next to the user-defined event times (the **Time Abs** column, highlighted in red), look for the summed times of all events. Take note of the **Time Abs** found on the line of the **Reinject from Pre-Store** event for performing the CCS calibration.

3.5. Fragment the targeted peak between the two rounds of IMS. Change the voltages of the reinjection step to increase the kinetic energy of the ions, and fragment them upon collision with the ion mobility gas.

3.5.1. Set the duration of the **Separate** event directly preceding the **Eject and Acquire** to 1 ms (see explanation in step 2.3.3).

3.5.2. On the **Reinject from Pre-Store** line, tick the **Enable Activation** box, and optimize the fragmentation with the built-in control. If the spectrum is satisfactory (e.g., the base peak is a fragment), proceed directly to step 3.5.4.

NOTE: When enabling activation, three voltages on the line will turn grey: these are the voltages that the user needs to change if manual optimization of the voltages is required (see the next step). These three voltages (**Pre-Array Gradient**, **Pre-Array Bias**, and **Array Offset**) form the gradient used to activate the ions. The kinetic energy of the ions will increase with the slope between the **Pre-Array Bias** and **Array Offset** (see **Figure 5**). The default values of the Gradient → Bias → Offset values are: without activation 85 → 70 → 45 V; maximum activation of the built-in function 185 → 170 → –5 V (+150 V). After fragmentation, do not forget to readjust the ion

transmission using the **DRE lens** (decrease the attenuation of the signal) (see step 3.2.).

3.5.3. If the fragmentation is not satisfactory with the built-in control, uncheck the **Enable Activation** box and proceed to manually optimize the reinjection voltages. Increase the **Pre-Array Gradient** voltage (the **Pre-Array Bias** voltage must always be kept 15 V below the **Pre-Array Gradient**), and lower the **Array Offset** voltage (which can be set as negative) until the results are satisfactory.

NOTE: When manually tuning the voltages of the multifunction array, the user can switch from the 'Mobilogram' view to interactive schematics of the voltages applied in the multifunction array (**PE diagram**) to better visualize the voltage settings (**Figure 5A**).

3.5.4. Record a 2 min acquisition. In the acquisition pop-up window, tick the **Retain Drift Time** option to generate a file containing only the arrival times vs *m/z* (the acquisition time used for chromatographic analyses—the retention time—is removed from the file). Note that this file is labeled ***_dt.RAW**.

NOTE: If the user forgets to check the **Retain Drift Time** option, it is still possible to extract the IMS dimension using the Driftscope 2.9 software (**File | Export to MassLynx | Retain Drift Time**).

3.6. Turn the instrument back to **TOF** mode in the main **Tune** page, and thoroughly rinse the system with 50:50 MeOH/H_2O before proceeding with the next sample.

4. IMS/IMS-MS processing with MZmine 2[24]

NOTE: MZmine 2 is available from the URL given in the **Table of Materials**. The use of MZmine 2.51 is recommended. At the time of preparation of this manuscript, the later versions cannot open RAW files from Cyclic IMS instruments because of a change in the import function.

4.1. Import the raw file(s) containing only the IMS and *m/z* dimensions (***_dt.RAW**) using **Raw data methods | Raw data import**.

NOTE: Raw files will appear on the left side of the main MZmine window. Do not import the original ***.RAW** files that still contain the retention time dimension. MZmine does not distinguish retention time from IMS arrival time, and the data points of both dimensions would overlap.

4.2. Optimize the workflow parameters on a representative file by selecting it in the **Raw data files** list.

4.2.1. Evaluate the noise level in the data. Right-click on the file in the **Raw data files** list, select **Show TIC** and display the base peak "chromatogram" (BPC). Double-click on the smallest peak observable by eye to display its mass spectrum. Consider the noise level in the data to be around that of the second isotope of the base peak in this spectrum, and use this same value for all the intensity thresholds in the following processing steps.

NOTE: The data were acquired using quadrupole isolation and are thus considered by MZmine as MS/MS. Throughout the entire MZmine processing, be sure to work at an **MS level = 2**.

4.2.2. Perform the mass detection using **Raw data methods | Feature detection | Mass detection**. For data acquired in profile mode, use the **Wavelet transform** algorithm. To set up the parameters of the algorithms in MZmine, click on the **[…]** button next to the algorithm and use the **Show preview** option to visualize the data while optimizing the parameters.

NOTE: At this stage, the peaks selected by the algorithm will appear in red in the preview window. When using the **wavelet transform** algorithm on proprietary RAW files, MZmine will sometimes mistake the profile data points for centroided peaks. The software will display a message stating that the user is running a profile algorithm on centroided spectra: ignore this message and click **OK**.

4.2.3. Reconstruct the extracted ion mobility spectra (EIM) for each fragment mass using **Raw data methods | Feature detection | ADAP Chromatogram builder** on the 'masses' mass list generated by the previous step. As the **m/z tolerance** input at this stage is a scan-to-scan tolerance, be sure to leave it at least 3–4 times higher than the overall expected accuracy.

4.2.4. As the previous step does not have a preview option, check the quality of the peak picking directly using the **Feature list** that appeared on the right panel of the main MZmine window. Open the **Feature list**, select all rows, right-click, and select **Show/XIC (dialog)**. Click **All** to display all ions on the mobility spectrum. Inspect the picked peaks that appear in color to ensure that there are no obvious missed peaks.

4.2.5. Deconvolve the EIMs to split the *m/z* that contain different peaks in multiple features. Use **Feature list methods | Feature detection | Chromatogram deconvolution**, and choose the **Wavelets (ADAP)** algorithm. Optimize the algorithm for the data using the **Show preview** option and the following key parameters: **S/N threshold**, **coefficient/area threshold**, and **RT wavelet range**.

NOTE: Checking the aspect of the deconvolved spectrum is recommended. Use the chromatogram visualization tool, as described in step 4.2.4. The deconvolved peaks will appear in color, and peaks of the same mass should be split, as presented in **Figure 6A**.

4.2.6. Deisotope the deconvolved EIMs using **Feature list methods | Isotopes | Isotopic peaks grouper**. Use the expected accuracy of the instrument for the *m/z* tolerance value, and set the arrival time tolerance to 0.1 ms (displayed in MZmine as **Retention time tolerance 0.1 min**), as isotopes are not resolved during the IMS separation. Check the feature list: if any isotopes remain, increase the tolerance values.

NOTE: Although the deisotoping can theoretically be performed at any moment of the feature list processing, it is important to do it last so that the charge values can be exported (the

algorithms used for the other steps will sometimes remove the charge state information).

4.3. If processing multiple IMS/IMS-MS spectra, repeat the processing with these optimized parameters. Keep the same parameters for all spectra.

4.4. In the case of multiple spectra, group them in a single table to export them; if not, skip directly to step 4.5. To group the spectra, use **Feature list methods | Alignment | Join aligner**. Because the objective is not to actually align the peaks, use restrictive tolerance values for both *m/z* and arrival time. Give the same weight to both dimensions.

4.5. Export the final feature list to a ***.csv** file. Use **Feature list methods | Export/Import | Export to CSV file** and export the following values: **Export row m/z, Export row retention time** (the actual IMS arrival time), **Peak m/z**, and **Peak height**. Use a comma as a field separator.

5. $^{TW}CCS_{N2}$ of the centroided IMS/IMS spectra

NOTE: In this protocol, a logarithmic fit calibration[25,26] will be used, which tends to give better results than linear calibration and is easy to implement in a spreadsheet or an in-house processing script. An in-house script (written in R) is available at the URL given in the **Table of Materials**.

5.1. Pick the reference arrival time values from the calibrant acquisition (see step 2.3). Do this manually using the constructor software (see the **Table of Materials**) to check the aspect of all IMS calibrant peaks.

5.1.1. In the **Chromatogram** window, open the ***_dt.RAW** file corresponding to the calibrant.

5.1.2. For each calibration point, generate the EIM using the **Display | Mass** option.

5.1.3. Check the profile of the EIMs. If some are poorly defined, smooth them using the **Process | Smooth** option (as the best results are typically obtained with the Savitzky-Golay algorithm, smooth 2 times over 3 bins). Report the apex values in a spreadsheet.

NOTE: Because the reference points are generally acquired using low-resolution DTIMS devices, some multimodal distributions may appear in Cyclic IMS depending on the calibrants. Remove any peak presenting such a distribution from the calibration list.

5.2. Calculate the logarithmic fit parameters from the calibrants.

5.2.1. For all calibration points, calculate the following.

5.2.1.1. Calculate the drift time using Eq (**1**):

$$t_d = t_A - t_{inj} \qquad (\mathbf{1})$$

with t_d the drift time, t_A the measured arrival time, and t_{inj} the time of injection in the IMS cell (all in ms).

NOTE: For small molecules, such as oligosaccharide fragments, the dead time (flight time between the exit from the IMS cell and the detector) variation between different masses is within the error range of the CCS calibration and can be ignored.

5.2.1.2. Calculate the neutral mass of the ions using Eq (**2**):

$$m_{neutral} = (m/z) \times |z| - m_{ion} \qquad (\mathbf{2})$$

with *z* the charge state of the ion, and m_{ion} the mass of the counter-ion (in Da). Use exact masses to avoid introducing uncertainty. If there is an atom loss instead of a counter-ion, use negative m_{ion} values (e.g., for $[M–H]^-$ $m_{neutral}$ *= (m/z) * |z| – (– 1.007276) = (m/z) * |z| + 1.007276*).

5.2.1.3. Calculate the CCS' parameter using Eq (**3**):

$$CCS' = \frac{CCS}{|z| \times \left(\frac{1}{m_{neutral}} + \frac{1}{m_{gas}}\right)^{0.5}} \qquad (\mathbf{3})$$

with *CCS* the reference drift tube $^{DT}CCS_{N2}$ value (in nm^2), and m_{gas} the mass of the drift gas (in Da; ex. for nitrogen: m_{gas} = 28.01 Da).

5.2.1.4. Calculate the t_d' parameter using Eq (**4**):

$$t'_d = t_d - 0.001 \times d \times (m/z)^{0.5} \qquad (\mathbf{4})$$

with *d* the detector start delay used experimentally to correct for dead time (typically ~1.5 ms).

5.2.1.5. Calculate logarithm of the above parameters: ln (*CCS'*) and ln (t'_d)

5.2.2. Perform a linear regression to determine the R^2 coefficient and the *x* and *y* parameters of the logarithmic fit (with *x* the slope and *ln(y)* the intercept) using Eq (**5**):

$$\ln(CCS') = x \times \ln(t'_d) + \ln(y) \qquad (\mathbf{5})$$

NOTE: The user can plot the ln(CCS') vs ln(t_d') values to visually check the results of the calibration, although this is optional.

5.3. Apply the calibration to the experimental data to calibrate the peaks picked by MZmine for every IMS/IMS spectrum exported to the *.csv file. For each point, calculate the following.

5.3.1. Calculate the drift time using Eq (**6**):

$$t_d = t_A - t_{seq} \quad (\mathbf{6})$$

with t_{seq} the time preceding the final IMS separation (the 'Time Abs' value noted in step 3.4.6).

NOTE: If calibrating multiple IMS/IMS spectra acquired with different sequences, carefully check the t_{seq} values.

5.3.2. Calculate the neutral mass of the ions using Eq (**7**):

$$m_{neutral} = (m/z) \times |z| - m_{ion} \quad (\mathbf{7})$$

5.3.3. Calculate the t_d' and t_d'' parameters using Eq (**8**) and Eq (**9**):

$$t'_d = t_d - 0.001 \times d \times (m/z)^{0.5} \quad (\mathbf{8})$$

$$t''_d = (t'_d)^x \times |z| \times \left(\frac{1}{m_{neutral}} + \frac{1}{m_{gas}}\right)^{0.5} \quad (\mathbf{9})$$

5.3.4. Calculate the final calibrated CCS values ($^{TW}CCS_{N2}$ in nm^2) using Eq (**10**):

$$^{TW}CCS_{N2} = t''_d \times y \quad (\mathbf{10})$$

NOTE: Although step 5.2.2. gives *ln(y)* as the intercept, *y* must be used to obtain the final CCS value. Do not forget to apply an exponential function.

5.4. Check the accuracy of the calibration by applying the calibration to the second acquisition of the calibration solution acquired in step 2.4.

NOTE: The calibration should yield results with an error of ~1–2%.

REPRESENTATIVE RESULTS:

An arabinoxylan pentasaccharide, XA^2XX, was chosen as an example to illustrate this protocol. This compound is commercially available, but only as a mixture with another arabinoxylan pentasaccharide, XA^3XX (pure XA^3XX is also commercially available). The structures of XA^2XX and XA^3XX are given in **Supplemental Figure S1**. As the ratio of XA^2XX and XA^3XX in the commercial mixture is ~50:50, a solution at 20 µg/mL of the mixture was prepared to reach an XA^2XX concentration of ~10 µg/mL in 50:50 MeOH/H_2O + 500 µM LiCl.

First, an MS analysis of the XA^2XX + XA^3XX mixture was performed using high-resolution MS. As the two compounds are isomers, a single peak was observed at $[M+Li]^+$ *m/z* 685.24. This MS peak was selected with the quadrupole and the selection window adjusted to remove the –1 Da lithium isotope, which could be mistaken as the monoisotopic peak by processing algorithms

(**Figure 2**).

The $[M+Li]^+$ adducts of the pentasaccharides were then submitted to the first stage of IMS separation: after 3 passes around the cyclic IMS cell, 3 peaks were separated with arrival times of 83, 90, and 94 ms. This profile was compared to that of pure XA^3XX (infused at 10 µg/mL), showing that the peaks at 83 and 90 ms corresponded to XA^3XX, while the peak at 94 ms corresponded to XA^2XX (**Figure 4A**). The peak at 94 ms was selected for IMS/IMS analysis: the ions belonging to XA^3XX were ejected (**Figure 4B**), and the peak of interest was sent to the prearray store cell. A 3-pass separation was performed after reinjecting the ion without activation to ensure that only the XA^2XX peak remained after the selection (arriving at 199 ms in **Figure 4C**).

Then, the ion was fragmented upon reinjection from the prestore area, and a single-pass IMS separation was performed on all the fragments. Two different activations were tried: the maximum setting of the built-in prestore activation function was first tried (**Figure 5B,C**); however, the precursor remained the base peak of the spectrum. This is not desired because, for reference spectra, fragments below a certain intensity threshold would typically be removed. Thus, a manually defined **prearray gradient → pre-array bias → array offset** voltage gradient was chosen (**Figure 5D,E**).

The generated IMS/IMS-MS data were deconvolved with MZmine 2.51, using the arrival time and *m/z* dimensions (**Figure 6A**), to give IMS/IMS spectra containing only the mobility information of the fragments. The peaks above 0.2% relative intensity were exported for CCS calibration (the detailed MZmine parameters are given in **Supplemental Table S1**). The CCS calibration was performed using the calibration solution (R^2 = 0.995, mean absolute deviation of control = 1.63%, see **Supplemental Table S3**). This processing finally afforded a centroided, CCS-calibrated, IMS/IMS spectrum (**Figure 6B**).

FIGURE AND TABLE LEGENDS:

Figure 1: Overview of the IMS/IMS data generation process. Abbreviations: IMS = ion mobility spectrometry; IMS/IMS = tandem IMS.

Figure 2: Isotopic pattern of an XA^3XX + XA^2XX arabinoxylan pentasaccharide mixture. (**A**) Saturated signal without DRE; (**B**) signal corrected using DRE with a 5% ion transmission (i.e., 95% attenuation); and (**C**) profile after quadrupole selection to remove the –1 Da peak corresponding to a lithium isotope. In purple: the region where artifact peaks can appear due to saturation is magnified 6 times. Abbreviations: DRE = dynamic range enhancement; MS = mass spectrometry; MSMS = tandem MS; LM Res = low-mass resolution; HM Res = high-mass resolution.

Figure 3: Overview of the Cyclic IMS control window, in which the user defines the IMS/IMS sequence. The sequence displayed shows how to check the quality of the isolation in IMS/IMS, with a selection of XA^2XX after 3 passes (the spectrum displayed corresponds to the setting of the selection events after the first-stage separation). The sequence consists in running a first 3-pass IMS separation over 58 ms, then ejecting the two faster isoforms from the IMS cell (segment

3), ejecting the slower isoform (ATD between 92 and 96 ms) in the prestore (segment 4), reinjecting it in the IMS cell without activation (segment 6), allowing the ions to undergo a further 3-pass (58-ms) separation (segment 7), then ejecting ions from the IMS cell, and acquiring data (segment 8). Abbreviations: IMS = ion mobility spectrometry; cIMS = cyclic IMS; IMS/IMS = tandem IMS; ADC = analog-to-digital converter; TW = traveling wave; PE = potential energy; ATD = arrival time distribution.

Figure 4: Selection of XA^2XX from the mixture of XA^2XX and XA^3XX. (**A**) Separation of the arabinoxylan pentasaccharides, XA^3XX and XA^2XX, after 3 passes (corresponding to a separation time set at 58 ms) around the Cyclic IMS cell. (**B**) Fraction ejected directly after the first stage of IMS separation. (**C**) Fraction selected for IMS/IMS on which another 3-pass separation was performed after reinjection. The XA^2XX peak of interest is highlighted in gray. The ion mobility spectra are shown in data bins and annotated with their arrival time (ms). Abbreviations: IMS = ion mobility spectrometry; IMS/IMS = tandem IMS.

Figure 5: Principles of collision-induced dissociation using the prearray store area. (**A**) Schematics of the multifunction array region detailing key voltages (in red) used for the selection, the reinjection, and the activation during IMS/IMS experiments. The blue arrows show the direction of the traveling wave in the multifunction array. (**B, C**) IMS/IMS and MS/MS spectra obtained for XA^2XX using the built-in prestore activation function (+150 V). The color bar represents the ion intensity scale (blue = low; red = high). (**D, E**) IMS/IMS and MS/MS spectra obtained for XA^2XX with manual optimization of the voltages (prearray gradient 195 V, prearray bias 180 V, array offset –10 V). Precursor ions are indicated by asterisks on the spectra. The ion mobility spectra are shown in data bins and annotated with their arrival time (ms). Abbreviations: IMS = ion mobility spectrometry; IMS/IMS = tandem IMS; TOF = time-of-flight.

Figure 6: Illustration of the processing steps. Results of (**A**) the MZmine peak picking and (**B**) the CCS calibration of arabinoxylan pentasaccharide XA^2XX. **A** shows the mass deconvolution of the IMS/IMS spectrum through a color code. **B** shows the final IMS/IMS spectrum after centroiding and CCS calibration. Abbreviations: IMS = ion mobility spectrometry; IMS/IMS = tandem IMS; CCS = collision cross section.

Figure 7: A comparison of two IMS/IMS spectra of XA^2XX illustrates the reproducibility of the method. The final calibrated spectrum from this paper (top) is compared to the spectrum from the work by Ollivier et al.[21] (bottom, flipped). Abbreviations: IMS = ion mobility spectrometry; IMS/IMS = tandem IMS; CCS = collision cross section.

Supplemental Figure S1: Structures of the XA^2XX and XA^3XX arabinoxylan pentasaccharides.

Supplemental Figure S2: Evaluation of the interday repeatability using XA^2XX. IMS/IMS acquisitions were repeated at Day 1 (top) and Day 95 (bottom). Abbreviations: IMS = ion mobility spectrometry; IMS/IMS = tandem IMS.

Supplemental Table S1: Detailed MZmine parameters.

Supplemental Table S2: Instrument parameters changed to evaluate the reproducibility. Abbreviation: ESI = electron spray ionization.

Supplemental Table S3: Control of the CCS calibration using a second acquisition of calibration solution.

DISCUSSION:

The SELECT SERIES Cyclic IMS is a powerful tool that allows selecting a defined ion population—of a given *m/z* and ion mobility—without the need for upstream chromatographic separation. The instrument affords the possibility of generating a bidimensional fragmentation map of this ion population, from which both MS/MS and IMS/IMS spectra can be extracted. However, the user must note several critical points that require attention during the experimental process.

First, the user should carefully check the MS isolation window for the presence of possible isobaric contaminants. Indeed, the isolation window of a quadrupole is relatively wide, and knowing ions of a slightly different *m/z* that may be coselected in the quadrupole will help the user properly assign the peak of interest in ion mobility.

Second, when performing the initial separation, the user must ensure that all ions undergo the same number of passes around the Cyclic ion mobility cell. This is an important and tricky aspect of ion mobility separation in a cyclic device. An erroneous evaluation of the number of passes for a given ion may lead to an improper identification and interpretation of the peaks. Controlling the number of passes of different ion populations can be tricky owing to the relatively short single-pass length (~1 m), and species with very different mobilities can quickly overlap.

In particular, a peak can split between two different passes if the array switches direction when this ion population passes through (this is relatively easy to identify: the split peak will appear sharper with a population right at the beginning of the **Eject and Acquire** event). To properly set the number of passes, the user should start with a short separation time (1–5 ms) that will give the 1-pass profile. Then, the user should gradually increase the separation time until the entire population has moved to higher arrival times, which will give the 2-pass profile. The 2-pass profile should look similar to the 1-pass profile but with better-resolved peaks. The time a given ion population takes to make one pass around the cyclic cell is a constant that the user can use to calculate the number of passes as a function of the separation time. For instance, if there is a 10 ms difference between the first and second pass, there will also be a 10 ms difference between the second and the third.

Third, during the IMS selection stage, the user should carefully check the quality of the isolation, as demonstrated in **Figure 4**. It is especially important to check the reinjected profile because if the TW height and velocity settings are too low, the ejection of the other populations might not be complete. Advanced users can correct this by adjusting the **Driftcell RF** radiofrequency voltage in the **RF** tab of the **Tune** page.

Fourth, the user should be careful in generating the fragmentation spectrum and, notably, in selecting the appropriate collision energy, especially if the voltages are tuned manually. Indeed, excessively lowering the **Array Offset** voltage can negatively impact the overall ion intensity by hindering the reinjection. In addition, the precursor and fragments might span over a wide range of mobilities. Thus, they will rapidly undergo a different number of passes if the final separation time is high, so it is important to keep a 1-ms **Separate** event as explained in protocol step 2.3.3. This is a major limitation since the single-pass length is relatively short, limiting the single-pass resolving power to ~100 for oligosaccharides[27]. In this respect, an increased path length in a single pass would be beneficial (i.e., the TWIMS-based Structures for Lossless Ion Manipulation or SLIM, with a path length of 13 m[28]). The SLIM setup was launched commercially very recently[29].

Finally, the user should be careful in defining the final acquisition mobility range using the **Pushes per bin** command, particularly if working on multiply charged ions. Ion mobility is indeed a function of the charge[12], and, for example, singly-charged fragments generated from a doubly-charged precursor are likely to be slower than the precursor (although they are smaller compounds).

A major limitation of using only MS and IMS separations to select the precursor (and not, for instance, an upstream step of chromatography) is that a given *m/z* can yield multiple peaks in IMS and that multiple peaks can come from the same compound. This is illustrated by the distributions of *m/z* 685.2, for both the XA^2XX+XA^3XX mixture and pure XA^3XX, in **Figure 4A**. Multimodal IMS distributions of a single *m/z* result from different gas-phase conformations. For species analyzed as cation adducts (in positive mode), the different conformations possibly arise from differences in coordination with the counter-ion[30–32].

For oligosaccharides, they can also arise from the separation of reducing-end anomers, although separating reducing-end anomers typically requires higher IMS resolving power than what is used here[33–35]. In the present case, the multimodal IMS distribution in **Figure 4A** results partly from the individual contributions of XA^2XX and XA^3XX. It is, however, notable that XA^3XX yields two peaks, which are likely cation-coordination conformers. It was easy to identify which peak corresponded to XA^2XX (i.e., the species of interest) because pure XA^3XX is available commercially, and its mobility profile could be recorded separately. To work on complex mixtures such as biological media, it may be important to consider adding a chromatographic separation stage.

Two points must be noted regarding the processing workflow used to obtain mass-deconvolved IMS/IMS spectra. First, in this protocol, it is proposed to use MZmine 2[24] to deconvolve the IMS/IMS spectrum using the MS dimension and, notably, use the ADAP algorithm[36] to split the EIMs into different peaks. Although it gives fairly good results, as illustrated in **Figure 6**, the ADAP algorithm was designed for chromatographic analyses and thus accounts for asymmetry factors inherent to liquid phase chromatography, such as peak tailing. Therefore, the ADAP algorithm might result in not identifying some of the features when applied to IMS peaks (e.g., shoulders). In essence, IMS data are simpler than chromatographic data: because there is no chemical

interaction of the compounds with a column, IMS data acquired under appropriate conditions (i.e., without saturating the IMS cell) are expected to follow gaussian distributions[37,38]. Ideally, the ADAP deconvolution step would be best replaced by a gaussian fitting function, such as that used by software destined for IMS like CUISuite 2[39]. However, as it stands, gaussian deconvolution was not directly adapted to the complete chain of treatment described in this protocol. Therefore, using the free, open-source software MZmine appeared to be a good compromise for end-users.

The second part of the processing that warrants discussion is the CCS calibration. This protocol proposes using a logarithmic fit calibration[25,26] and a commercial calibrant mixture from the same provider as that of the spectrometer (see the **Table of Materials**). This procedure is the most straightforward to implement in the lab. Regarding the choice of the calibrant mixture, the user should consider that, as mentioned in several studies, the accuracy of the CCS calibration is improved when using calibrants of the same molecular class and charge state as the analyte[26,40,41]. The error introduced when calibrating with relatively similar types of compounds (e.g., carbohydrates vs. peptides) is moderate. However, it is recommended not to use very different ions such as, for example, using salt clusters as calibrants when measuring carbohydrates[41]. Regarding the choice of the calibration method, Richardson et al.[42] recently reported a new calibration method that takes into account the physics of TWIMS to improve the accuracy of the calibration (with a provided software). However, the approach requires the evaluation of highly specific parameters through the analysis of various types of compounds—ranging from metabolites to native proteins. Because no mixture of such a variety of compounds can be found commercially, this method was not implemented in the present protocol.

Finally, to evaluate the reproducibility of the method, we evaluated the interday reproducibility by repeating the IMS/IMS-MS acquisition at day 1 and day 95 (**Supplemental Figure S2**). The experiment showed that IMS/IMS-MS data are highly reproducible, with no IMS peak shifting by more than 0.2 ms over this extended period. The IMS/IMS spectrum generated in this work was further compared to another spectrum of XA^2XX acquired under different conditions for previous work on ion mobility-molecular networking[21]. Some instrumental parameters that can impact the ion structure and ion mobility profile[13] were deliberately changed—the source parameters and the activation voltage gradient (a comparison of the varying instrumental conditions is given in **Supplemental Table S2**). Then, the two spectra were compared using the cosine similarity score—which is popular for the comparison of MS/MS spectra in metabolomics—on the GNPS platform[5] (CCS tolerance for matching fragments = 0.015 nm^2).

The comparison showed a cosine similarity score of 0.87 (**Figure 7**), which can be considered high with regard to the important instrumental variations applied. This leads to the idea that IMS/IMS spectral libraries could be used to dereplicate glycans in complex mixtures with a high level of confidence, which would not be the case with MS/MS spectra. Note that although the current approach only uses the CCS dimension of the fragmentation spectrum, the IMS/IMS-MS data also contains MS information, which is not redundant with the CCS. To optimize the dereplicative power of IMS/IMS, a bidimensional scoring system must be developed.

ACKNOWLEDGMENTS:

S.O. is thankful to the French National Research Agency for funding his Ph.D. (grant ANR-18-CE29-0006).

DISCLOSURES:

The authors have no conflict of interest to disclose.

REFERENCES:

1. Allard, P. -M. et al. Integration of molecular networking and in-silico MS/MS fragmentation for natural products dereplication. *Analytical Chemistry*. **88** (6), 3317–3323 (2016).
2. Wang, M. et al. Mass spectrometry searches using MASST. *Nature Biotechnology*. **38** (1), 23–26 (2020).
3. David, M., Fertin, G., Rogniaux, H., Tessier, D. SpecOMS: a full open modification search method performing all-to-all spectra comparisons within minutes. *Journal of Proteome Research*. **16** (8), 3030–3038 (2017).
4. Dührkop, K. et al. SIRIUS 4: a rapid tool for turning tandem mass spectra into metabolite structure information. *Nature Methods*. **16** (4), 299–302 (2019).
5. Wang, M. et al. Sharing and community curation of mass spectrometry data with Global Natural Products Social Molecular Networking. *Nature Biotechnology*. **34** (8), 828–837 (2016).
6. Nothias, L.-F. et al. Feature-based molecular networking in the GNPS analysis environment. *Nature Methods*. **17** (9), 905–908 (2020).
7. Gray, C. J. et al. Advancing solutions to the Carbohydrate Sequencing Challenge. *Journal of the American Chemical Society*. **141** (37), 14463–14479 (2019).
8. Ropartz, D. et al. Online coupling of high-resolution chromatography with extreme UV photon activation tandem mass spectrometry: Application to the structural investigation of complex glycans by dissociative photoionization. *Analytica Chimica Acta*. **933**, 1–9 (2016).
9. Wolff, J. J. et al. Negative electron transfer dissociation of glycosaminoglycans. *Analytical Chemistry*. **82** (9), 3460–3466 (2010).
10. Ropartz, D. et al. Charge transfer dissociation of complex oligosaccharides: comparison with collision-induced dissociation and extreme ultraviolet dissociative photoionization. *Journal of the American Society for Mass Spectrometry*. **27** (10), 1614–1619 (2016).
11. Morelle, W. et al. Fragmentation characteristics of permethylated oligosaccharides using a matrix-assisted laser desorption/ionization two-stage time-of-flight (TOF/TOF) tandem mass spectrometer. *Rapid Communications in Mass Spectrometry*. **18** (22), 2637–2649 (2004).
12. Gabelica, V., Marklund, E. Fundamentals of ion mobility spectrometry. *Current Opinion in Chemical Biology*. **42**, 51–59 (2018).
13. Gabelica, V. et al. Recommendations for reporting ion mobility mass spectrometry measurements. *Mass Spectrometry Reviews*. **38** (3), 291–320 (2019).
14. Hernandez-Mesa, M. et al. Interlaboratory and interplatform study of steroids collision cross section by traveling wave ion mobility spectrometry. *Analytical Chemistry*. **92** (7), 5013–5022 (2020).
15. Koeniger, S. L. et al. An IMS−IMS analogue of MS−MS. *Analytical Chemistry*. **78** (12), 4161–4174 (2006).

16. Merenbloom, S. I., Koeniger, S. L., Valentine, S. J., Plasencia, M. D., Clemmer, D. E. IMS−IMS and IMS−IMS−IMS/MS for separating peptide and protein fragment ions. *Analytical Chemistry*. **78** (8), 2802–2809 (2006).
17. Eldrid, C., Thalassinos, K. Developments in tandem ion mobility mass spectrometry. *Biochemical Society Transactions*. **48** (6), 2457–2466 (2020).
18. Giles, K. et al. A cyclic ion mobility-mass spectrometry system. *Analytical Chemistry*. **91** (13), 8564–8573 (2019).
19. Merenbloom, S. I., Glaskin, R. S., Henson, Z. B., Clemmer, D. E. High-resolution ion cyclotron mobility spectrometry. *Analytical Chemistry*. **81** (4), 1482–1487 (2009).
20. Ollivier, S. et al. Anomeric retention of carbohydrates in multistage cyclic ion mobility (IMSn): de novo structural elucidation of enzymatically produced mannosides. *Analytical Chemistry*. **93** (15), 6254–6261 (2021).
21. Ollivier, S., Fanuel, M., Rogniaux, H., Ropartz, D. Molecular networking of high-resolution tandem ion mobility spectra: a structurally relevant way of organizing data in glycomics? *Analytical Chemistry*. **93** (31), 10871–10878 (2021).
22. Aron, A. T. et al. Reproducible molecular networking of untargeted mass spectrometry data using GNPS. *Nature Protocols*. **15** (6), 1954–1991 (2020).
23. McKenna, K. R., Li, L., Krishnamurthy, R., Liotta, C. L., Fernández, F. M. Organic acid shift reagents for the discrimination of carbohydrate isobars by ion mobility-mass spectrometry. *The Analyst*. **145** (24), 8008–8015 (2021).
24. Pluskal, T., Castillo, S., Villar-Briones, A., Orešič, M. MZmine 2: Modular framework for processing, visualizing, and analyzing mass spectrometry-based molecular profile data. *BMC Bioinformatics*. **11**, 395 (2010).
25. Ruotolo, B. T., Benesch, J. L. P., Sandercock, A. M., Hyung, S. -J., Robinson, C. V. Ion mobility–mass spectrometry analysis of large protein complexes. *Nature Protocols*. **3** (7), 1139–1152 (2008).
26. Bush, M. F., Hall, Z., Giles, K., Hoyes, J., Robinson, C. V., Ruotolo, B. T. Collision cross sections of proteins and their complexes: a calibration framework and database for gas-phase structural biology. *Analytical Chemistry*. **82** (22), 9557–9565 (2010).
27. Ropartz, D. et al. Structure determination of large isomeric oligosaccharides of natural origin through multipass and multistage cyclic traveling-wave ion mobility mass spectrometry. *Analytical Chemistry*. **91** (18), 12030–12037 (2019).
28. Tolmachev, A. V. et al. Characterization of ion dynamics in structures for lossless ion manipulations. *Analytical Chemistry*. **86** (18), 9162–9168 (2014).
29. Arndt, J. R. et al. High-resolution ion-mobility-enabled peptide mapping for high-throughput critical quality attribute monitoring. *Journal of the American Society for Mass Spectrometry*. **32** (8), 2019–2032 (2021).
30. Le Fèvre, A., Dugourd, P., Chirot, F. Exploring conformational landscapes using trap and release tandem ion mobility spectrometry. *Analytical Chemistry*. **93** (9), 4183–4190 (2021).
31. Ohshimo, K., He, X., Ito, R., Misaizu, F. Conformer separation of dibenzo-crown-ether complexes with Na^+ and K^+ ions studied by cryogenic ion mobility-mass spectrometry. *The Journal of Physical Chemistry A*. **125** (17), 3718–3725 (2021).
32. Purves, R. W., Barnett, D. A., Ells, B., Guevremont, R. Gas-phase conformers of the [M + 2H]2+ ion of bradykinin investigated by combining high-field asymmetric waveform ion mobility

spectrometry, hydrogen/deuterium exchange, and energy-loss measurements. *Rapid Communications in Mass Spectrometry*. **15** (16), 1453–1456 (2001).
33. Ujma, J. et al. Cyclic ion mobility mass spectrometry distinguishes anomers and open-ring forms of pentasaccharides. *Journal of the American Society for Mass Spectrometry*. **30** (6), 1028–1037 (2019).
34. Warnke, S., Faleh, A. B., Scutelnic, V., Rizzo, T. R. Separation and identification of glycan anomers using ultrahigh-resolution ion-mobility spectrometry and cryogenic ion spectroscopy. *Journal of The American Society for Mass Spectrometry*. **30** (11), 2204–2211 (2019).
35. Williamson, D. L., Bergman, A. E., Nagy, G. Investigating the structure of α/β carbohydrate linkage isomers as a function of group I metal adduction and degree of polymerization as revealed by cyclic ion mobility separations. *Journal of the American Society for Mass Spectrometry*. **32** (10), 2573–2582 (2021).
36. Myers, O. D., Sumner, S. J., Li, S., Barnes, S., Du, X. One step forward for reducing false positive and false negative compound identifications from mass spectrometry metabolomics data: new algorithms for constructing extracted ion chromatograms and detecting chromatographic peaks. *Analytical Chemistry*. **89** (17), 8696–8703 (2017).
37. Marchand, A., Livet, S., Rosu, F., Gabelica, V. Drift tube ion mobility: how to reconstruct collision cross section distributions from arrival time distributions? *Analytical Chemistry*. **89** (23), 12674–12681 (2017).
38. Davis, D. M. et al. Analysis of ion mobility spectra for mixed vapors using Gaussian deconvolution. *Analytica Chimica Acta*. **289** (3), 263–272 (1994).
39. Polasky, D. A., Dixit, S. M., Fantin, S. M., Ruotolo, B. T. CIUSuite 2: next-generation software for the analysis of gas-phase protein unfolding data. *Analytical Chemistry*. **91** (4), 3147–3155 (2019).
40. Salbo, R. et al. Traveling-wave ion mobility mass spectrometry of protein complexes: accurate calibrated collision cross-sections of human insulin oligomers. *Rapid Communications in Mass Spectrometry*. **26** (10), 1181–1193 (2012).
41. Gelb, A. S., Jarratt, R. E., Huang, Y., Dodds, E. D. A study of calibrant selection in measurement of carbohydrate and peptide ion-neutral collision cross sections by traveling wave ion mobility spectrometry. *Analytical Chemistry*. **86** (22), 11396–11402 (2014).
42. Richardson, K., Langridge, D., Dixit, S. M., Ruotolo, B. T. An improved calibration approach for traveling wave ion mobility spectrometry: robust, high-precision collision cross sections. *Analytical Chemistry*. **93** (7), 3542–3550 (2021).

Figure 1

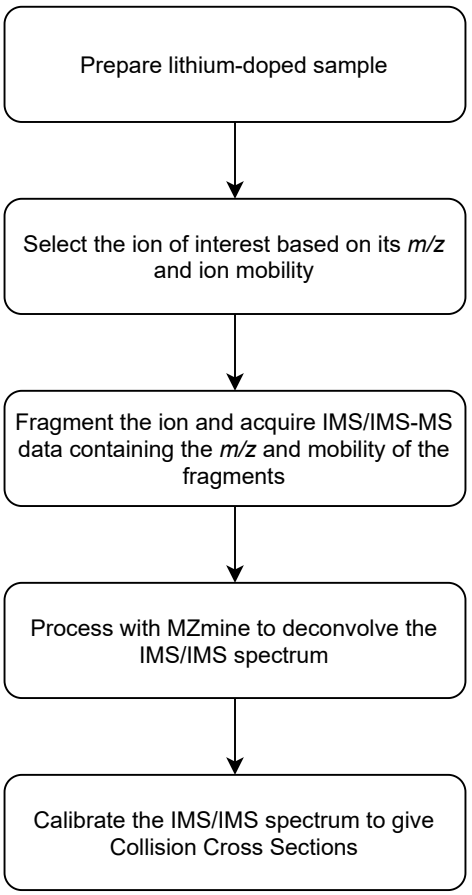

Figure 2

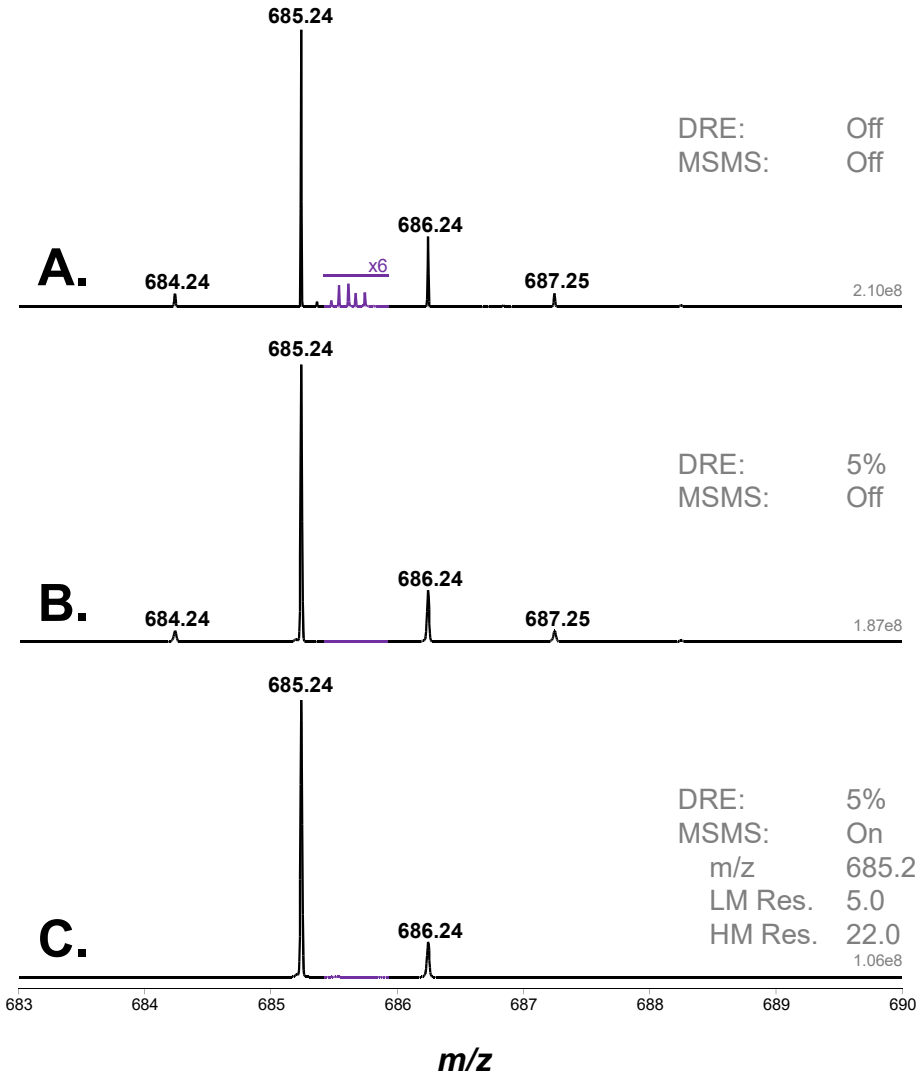

Figure 3

Click here to access/download;Figure;Figure3.pdf

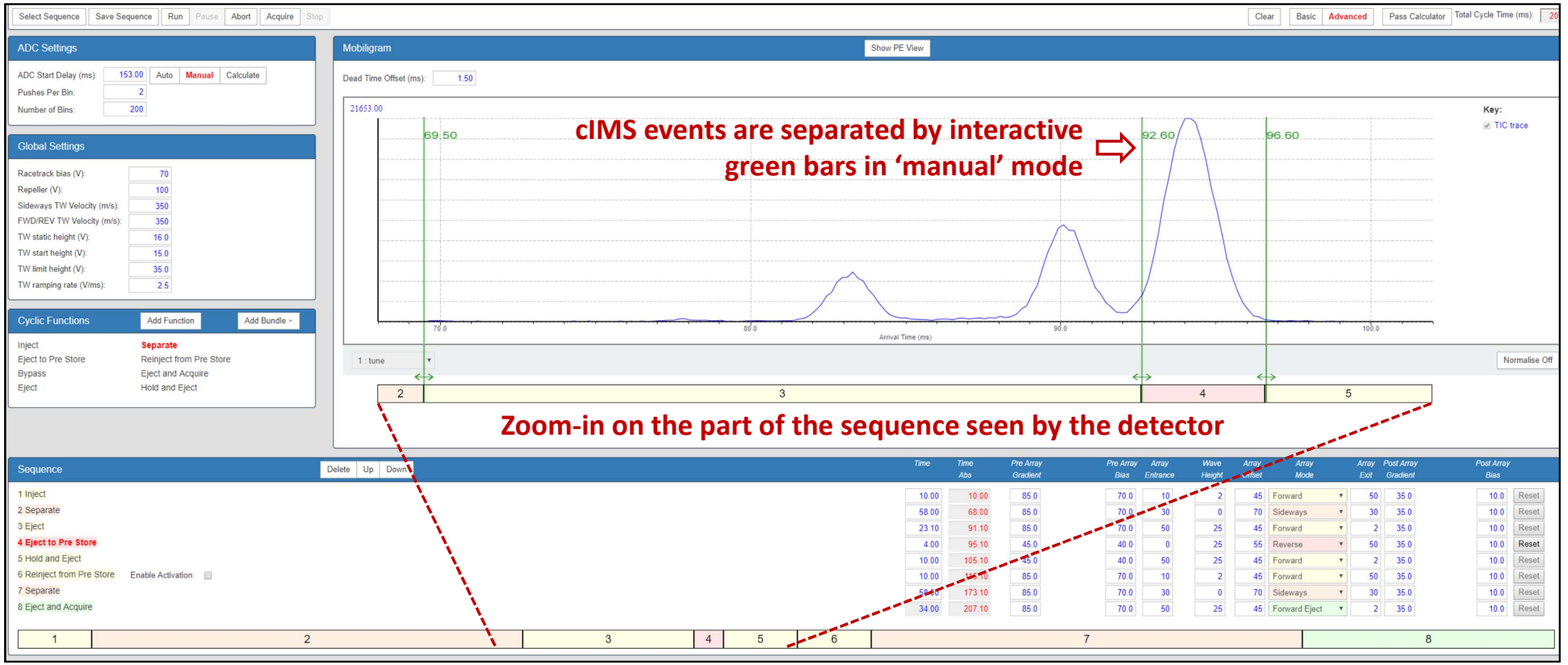

Figure 4

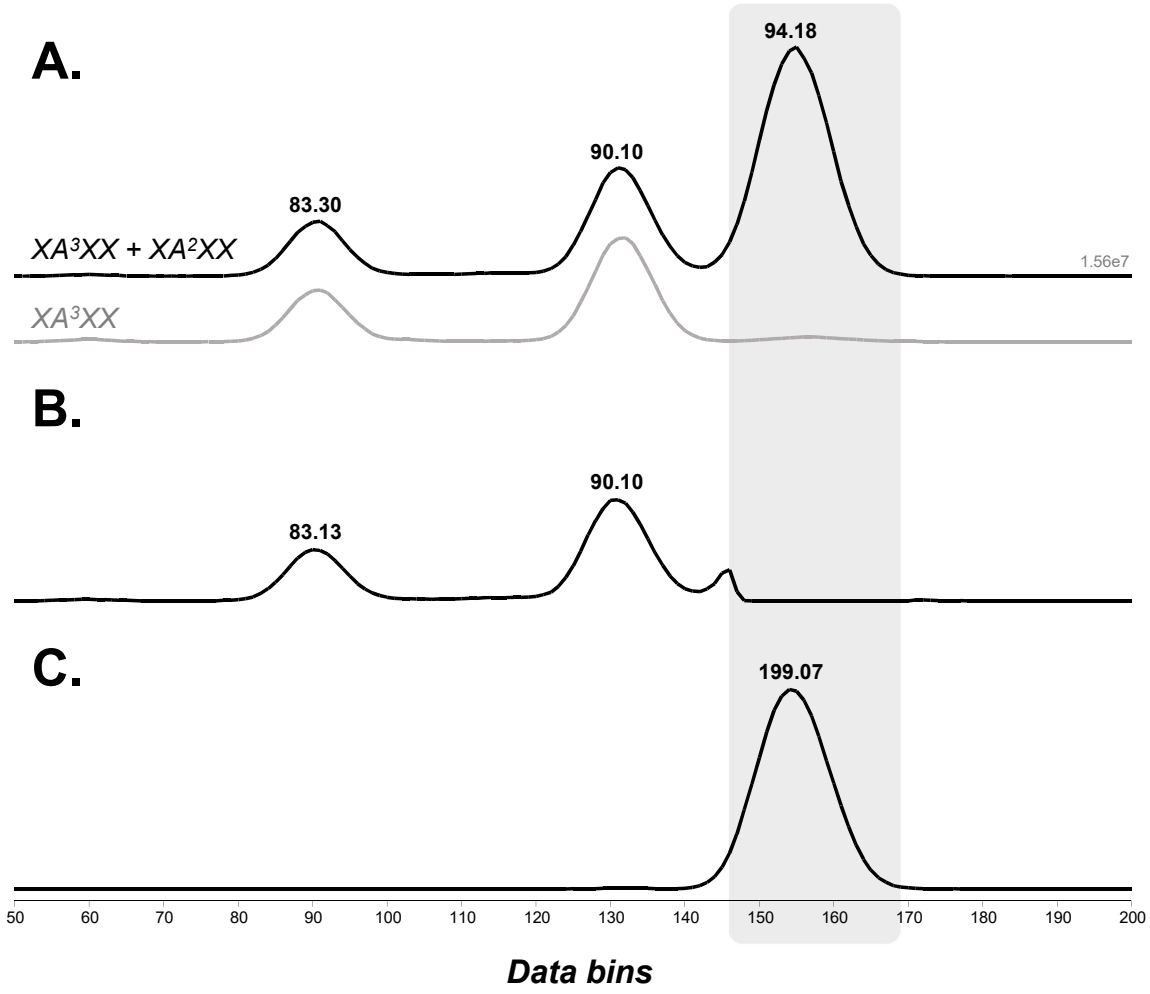

Figure 5

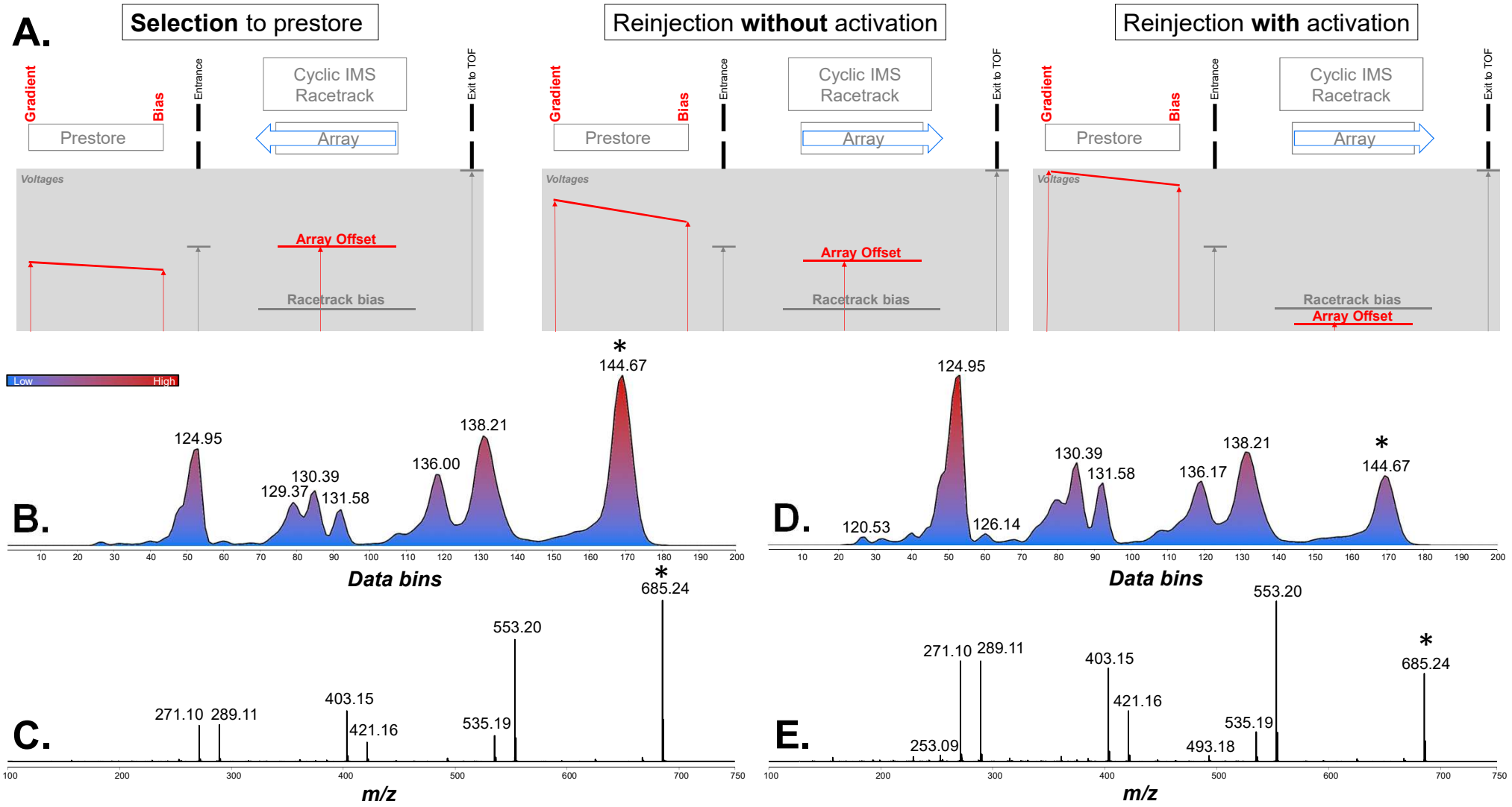

Figure 6

Click here to access/download;Figure;Figure6.pdf

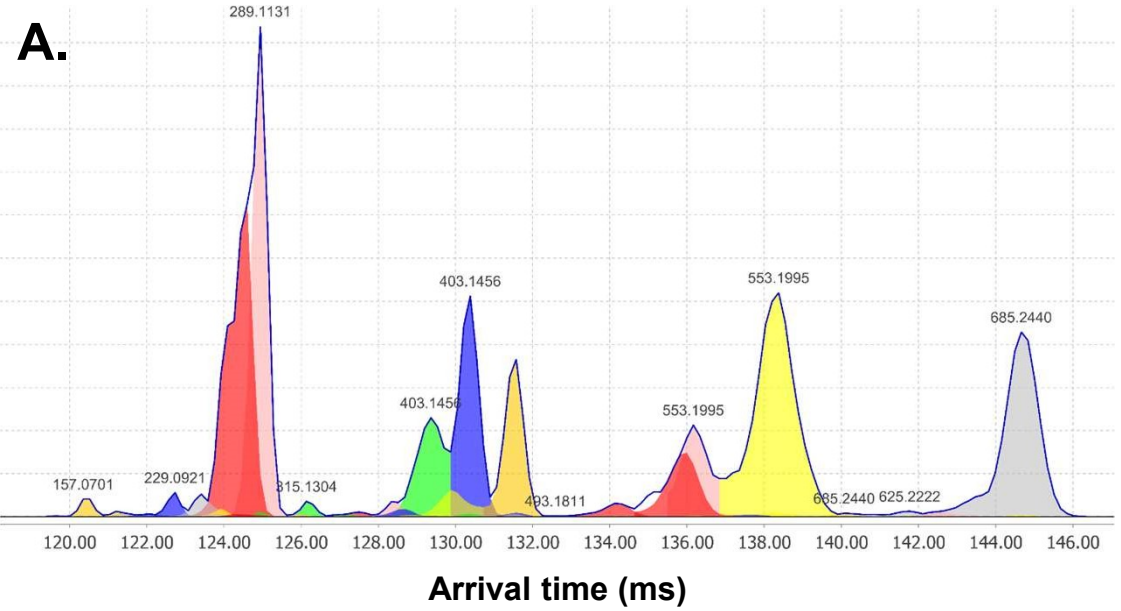

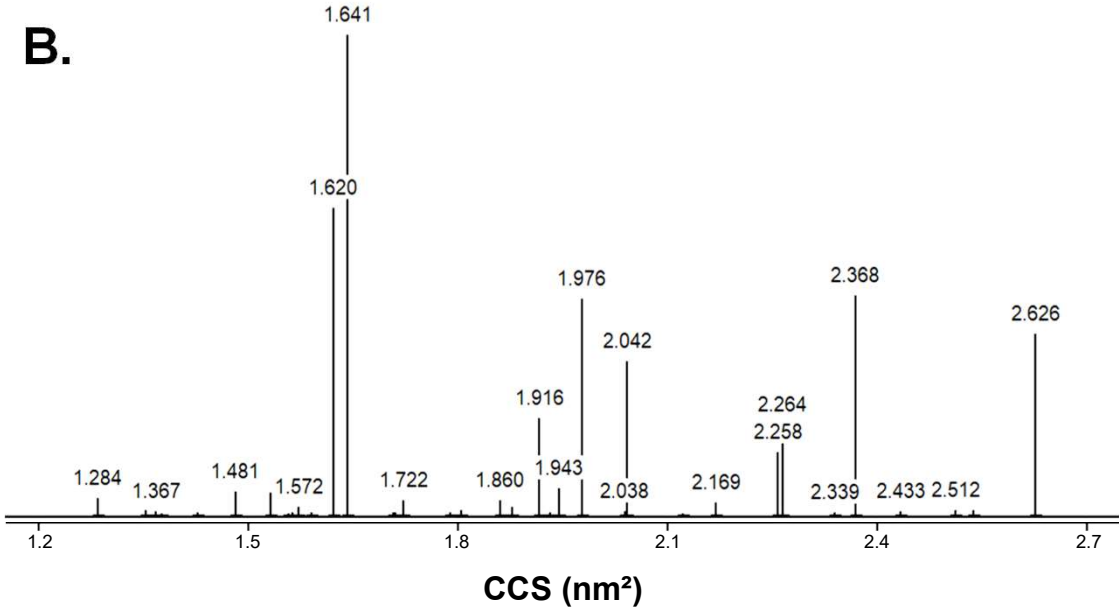

Figure 7

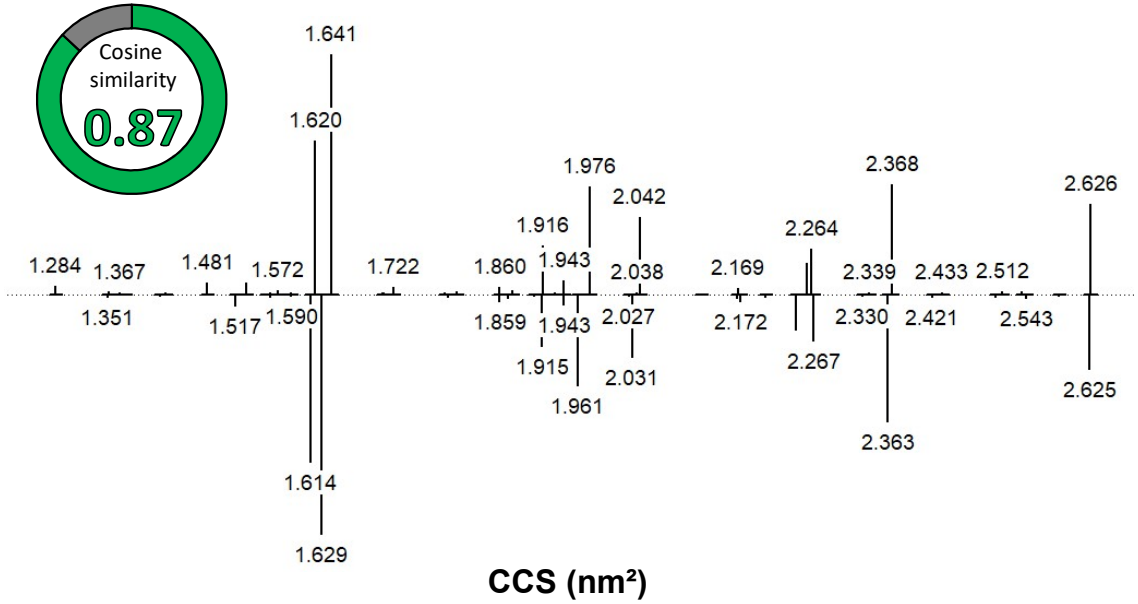

December 17, 2021

Dear Dr. Jana,

We are honoured that the reviewers have considered the interest of our protocol for a publication in the *Journal of Visualized Experiments*. We would like to thank you and the reviewers for your constructive comments that have substantially improved the paper.

We hope that we have satisfactorily addressed the different points and that the revised manuscript is now acceptable for publication.

Below you will find our answers to the editorial comments and to the reviewers' comments.

Among the main changes:

- We have added some discussion regarding the practical limitations of the protocol/instrumentation.
- We have performed an additional experiment to further validate the reproducibility of the method, shown in a new supplementary Figure S2.
- More detail was added to the protocol steps to answer the "how" question, and the protocol was clarified to contain only 2-3 actions per step.

A revised version of the manuscript with tracked changes is provided, along with a revised version of the table of material and the individual files for all supplementary Figures and Tables.

Sincerely,

Editorial comments:

Editorial changes to be made by Authors:

1. Please take this opportunity to thoroughly proofread the manuscript to ensure that there are no spelling or grammar issues.

Done.

2. Please revise the text to avoid the use of any personal pronouns (e.g., "we", "you", "our" etc.).

Done. Please note that we have left personal pronouns when refering to our previous work in the abstract and introduction.

3. Please remove the journal citation, commercial instrument name, and numbering within the Abstract. Rephrase the Abstract into a single paragraph clearly stating the goal of the protocol.

Remove citation, commercial instrument name and numbering: Done.

Rephrase the abstract: From our point of view, the goal of the protocol was already contained in the abstract. We have modified the phrasing to highlight which part is the actual goal.

4. For in-text formatting, corresponding reference numbers should appear as numbered superscripts before the punctuation.

Done.

5. JoVE cannot publish manuscripts containing commercial language. This includes trademark symbols (™), registered symbols (®), and company names before an instrument or reagent. Please remove all commercial language from your manuscript and use generic terms instead. All commercial products should be sufficiently referenced in the Table of Materials (e.g., Waters Corp., Falcon, Eppendorf, MassLynx 4.2).

Done. Note that the term ‘MassLynx’ occurs once in a click-button command and was left as is in this case.

6. Please use Calibri font throughout the manuscript and highlight all the windows, menus, and commands in Bold (non-italic).

Done.

7. Please ensure that all text in the protocol section is written in the imperative tense as if telling someone how to do the technique (e.g., “Do this,” “Ensure that,” etc.). Avoid usage of phrases such as “could be,” “should be,” and “would be” throughout the Protocol. Any text that cannot be written in the imperative tense may be added as a “Note.”

Done.

For the detail of information moved to notes, see point #9 where all modifications applied to the protocol are described.

8. Please add more details to your protocol steps. Please ensure you answer the “how” question, i.e., how is the step performed?

a. Step 1.2: Please specify the amount (in mg) of carbohydrate used.

Done. 1 mg.

b. Steps 2.1, 3.2: Please include details of pages, tabs, etc. associated with putting the instrument in the desired mode.

Step 2.1. Specified 'MS tune page'

Step 3.2. Specified that this must be done from the MS tune page

c. Step 2.2: Please mention how to infuse solutions in the ion source.

Added a note to specify that this must be done through the fluidics system of the instrument.

d. Step 2.3.1: is a syringe pump used for infusing? how to control the flow rate? Please provide details.

Specified that this must be done through the fluidics system.

e. Step 2.3.3: Please rephrase the text to contain action steps in the imperative tense. Also, please mention the tab containing the specified events in italic.

Done.

f. Steps 2.3.4, 2.4: Please provide button clicks for recording acquisitions.

Done.

g. Step 3.3: Please provide details of a tab or field for entering the selected mass of the ion.

Done.

9. Please simplify the Protocol so that individual steps contain only 2-3 actions per step and a maximum of 4 sentences per step. Please use a single line spacing between steps and sub-steps of the protocol.

Step 2.2.2 split in 2.2.2 + 2.2.3

Step 3.4.3. Description moved to a note

Step 3.4.4. Description moved to a note

Step 4.1. Description moved to a note

Step 4.2.1 phrasing changed to 4 sentences

Step 5.2.1. split in 5.2.1.1. through 5.2.1.5.

Step 5.3. split in 5.3.1. through 5.3.4. + description moved to a note in 5.3.1.

Note that from a mass spectrometrist point of view, it is usual to have a single action containing multiple clicks in the control software.

10. Please move websites to the Table of Materials and refer to it in the manuscript wherever required.

Done.

11. Figures 4-6: please include one-liner titles in the legends.

Done.

12. Figure 7: Please obtain explicit copyright permission to reuse any figures from publication. Explicit permission can be expressed in the form of a letter from the editor or a link to the editorial policy that allows re-prints. Please upload this information as a .doc or .docx file to your Editorial Manager account. The Figure must be cited appropriately in the Figure Legend, i.e. “This figure has been modified from [citation].”

We certify that Figure 7 has not been reused nor adapted from the previous publication. One of the two spectra shown in Figure 7 is part **of the data** used in our previous study, but the spectrum itself was not included in any graphics or figure. As such, **it is not subject to copyright** of the ACS.

13. Please remove numbering in the Discussion section.

Done.

14. Please submit individual Supplementary Figures and Supplementary Tables as separate files to your Editorial Manager account. Include the corresponding legends in the Figure Legends section of the manuscript.

Done.

Reviewers' comments:

Reviewer #1:

Manuscript Summary:

The authors describe a protocol for analyzing a lithiated pentasacharide using IMS/IMS on a Waters Select cIMS, and the associated data processing. Overall, the paper is well-written and easy to follow (even though I have only used the cIMS on one occasion). I suggest acceptance following minor revisions below, mostly making mention of some practical limitations of the current instrumentation/protocol.

Major Concerns:

1. P4 L 98: "increase nearly infinitely" - Nice in theory, but the length of your separations will always be limited by your (1 m) path length. This practical limitation should be mentioned, especially as it pertains to different mobility ranges; for example, species with very similar mobility will be able to undergo considerably more passes before lapping, than those species with very different mobility. Is there a practical limit you have observed? 50 m? 100 m? You could also mention that increasing that path length of a single pass (i.e., 13-m SLIM) could accommodate a wider range of mobility.

We have specified in the introduction that this is theoretical:

> “The cyclic IMS cell theoretically allows increasing near infinitely the drift path length”

We have further discussed the limitation of the 1-m separation in the discussion (see below).

Note that the problem of different mobility ranges is not a major concern for the separation of different species, as species with a different mobility can be sequentially ejected from the

mobility cell until only the species of interest is selected with a high resolution. As such, we have previously been able to perform separations over 100 m on standards.

The single-pass length limitation is thus mainly a concern when performing an IMS separation over a wide range of ions, for instance here the fragments in IMS/IMS. This limits the separation to a single pass, as it is practically impossible to keep all fragments in the same pass otherwise.

> "Second, when performing the initial separation, the user must make sure that all ions are undergoing the same number of passes around the Cyclic ion mobility cell. This is an important and tricky aspect of ion mobility separation in a cyclic device. An erroneous evaluation of the number of passes for a given ion may lead to an improper identification and interpretation of the peaks. Controlling the number of passes of different ion populations can be tricky owing to the relatively short single-pass length (*ca*. 1 m), and species with very different mobilities can quickly overlap. Especially, a peak can split between two different passes if the array switches direction when this ion population is passing through (this is relatively easy to identify: the split peak will appear sharper with a population right at the beginning of the Eject and Acquire event). […]
>
> Fourth, the user should be careful in generating the fragmentation spectrum, and notably in selecting the appropriate collision energy, especially if the voltages are tuned manually. Indeed, excessively lowering the Array Offset voltage can negatively impact the overall ion intensity by hindering the reinjection. In addition, the precursor and fragments might span over a wide range of mobilities. Thus, they will rapidly undergo a different number of passes if the final separation time is high, so it is important to keep a 1-ms Separate event as explained in point 2.3.3. This is a major limitation since the single-pass length is relatively short, limiting the single-pass resolving power to *ca.* 100 for oligosaccharides[27]. In this respect, an increased path length in a single pass would be beneficial (i.e., the TWIMS-based Structures for Lossless Ion Manipulation or SLIM, with a path length of 13 m[28]). The SLIM setup was launched commercially very recently[29]."

2. There should be a practical discussion of fluctuation in temperature/pressure as a function of separation length. How reproducible are arrival times for a given species, such as your sugar, when the same experiment is repeated several times? What about day-to-day variability?

We have added some discussion about the relationship between pressure, temperature, and length in IMS in the introduction (to date, we have not observed any phenomena of collisional heating during cIMS separation of oligosaccharides):

> "The low-field methods allow access to a so-called Collision Cross Section (CCS), a property of the ion-gas pair that represents the surface (in Å^2 or nm^2) of the ion that interacts with the buffer gas during the separation. CCS is theoretically instrument-independent, and is thus useful to generate data that can be reproduced between different laboratories. Ion mobility separations can be impacted by various parameters, and notably by fluctuations of the gas pressure and gas temperature in the mobility cell. The CCS calibration is a way to remedy this, as both the calibrant and the species of interest will be similarly affected[13]. However, it is mandatory to install the instrument in a temperature-controlled room and to have a reliable gas pressure control system."

Regarding pressure, the cyclic IMS operates at 1.75 mbar of N_2. Regarding temperature, the Cyclic IMS unfortunately does not give a readback of the temperature in the drift region. To

limit the variations in gas temperature, we have placed our instrument in a thermostated lab (20 °C). All of this has been specified in a note placed at the early steps of the protocol:

> "NOTE: For the best reproducibility, the voltages in the IMS cell need to be completely stabilized. Turn on the high voltages and let the instrument stabilize overnight before any cyclic IMS analysis. Furthermore, the pressure and temperature in the ion mobility cell must be kept as constant as possible. A readback for the pressure is available in the "**Vacuum**" tab, but no readback is available for the temperature. Keep the instrument in a thermostated lab. The instrument used in this work operates at 1.75 mbar in a lab thermostated at 20 °C."

Finally, we have evaluated day-to-day variability by repeating the IMS/IMS experiment for XA^2XX. The arrival time distributions are presented in the new **Figure S2**, illustrating the high repeatability of the measurement. Indeed, no peak in the IMS/IMS spectrum of XA^2XX shifted by more than 0.2 ms after 95 days.

3. I am concerned about CCS measurement for multi-pass separations. Are you including your calibrant ions in the same sample, or doing separate measurements? If the latter, how sure you can be there is no fluctuation in temp/pressure that could influence arrival time (see previous comment)? Does performing longer separations require calibrants with a narrower mobility range to both (a) still bracket your ions of interest, and (b) not lead to lapping of the calibrants?

In this protocol, we only perform CCS calibration for the final IMS/IMS spectrum, which was limited to a single-pass separation because of the above-mentioned limitations (see also our answer to question 1). As such, we are not performing any multi-pass CCS calibration, but it would indeed be tricky to calibrate a wide range of ions such as in the fragmentation spectra over multiple passes. Probably, a judicious choice of the calibrant would then be necessary in order to both bracket all the fragments and avoid the wrap-around, like the Reviewer said. In the arrival time distributions shown in the paper, the peaks are annotated with their arrival times (in ms). This has now been specified in the figure legends.

Regarding the calibrant, we use a commercial calibration mixture (Waters majormix). We acquire two IMS-MS spectra of the calibrant (independently from the samples to avoid ionization competition and any ion-ion interaction). We use one acquisition for the calibration and the other as control to check the consistency of arrival times/CCS between independent acquisitions, as shown in steps 2.3. and 5. of the protocol, and in Table S2.

4. You mentioned these networks (IMS-MN) but then make no discussion of this in the protocol and/or in the Discussion. An appropriate discussion should be included, otherwise you can simply mention that you don't consider the IMS-MN in this protocol paper.

The objective of this protocol is in fact not to build networks, but rather to explain how to generate IMS/IMS data, that users can then use to build networks—or for any other application of their choice. We have added the following statement in the manuscript, at the end of the introduction:

> "[…] In order to complement this publication and help Cyclic IMS users implement this workflow, this protocol provides a complete description of the protocol used to collect the data. This protocol focuses only on the generation of the IMS/IMS data that users can then use to build IM-MN networks (like we did in a previous published work[21])—or for any other application of their choice. Building of IM-MN will not be considered herein, as protocols for molecular networking are already available[22]. The crucial points that

must be followed to generate valuable and reproducible IMS/IMS acquisitions are highlighted. […]”

Minor Concerns:

- P4 L90: There were actually two Clemmer papers that should be cited, both in Analytical Chemistry in 2006, one by Koeniger (referenced) and the other by Merenbloom.

The missing reference has been added.

Reviewer #2:

Manuscript Summary:

Describing this new separations protocol using the Synapt cyclic IMS is certainly a unique application and this will be available to help new users to apply this type of method. The article is well organized and described and I recommend publication of the article and video. Overall, the manuscript does not need any major changes just a few minor typos I noticed as reading through.

Major Concerns:

None

Minor Concerns:

Typos

Line

140 1.2. In an Eppendorf tube, weigh a low-mg amount of the carbohydrate.

Corrected

217 multitude of low-abundance peaks in-between isotopes.

Corrected

600 case with MS/MS spectra. Note that our current approach

Corrected

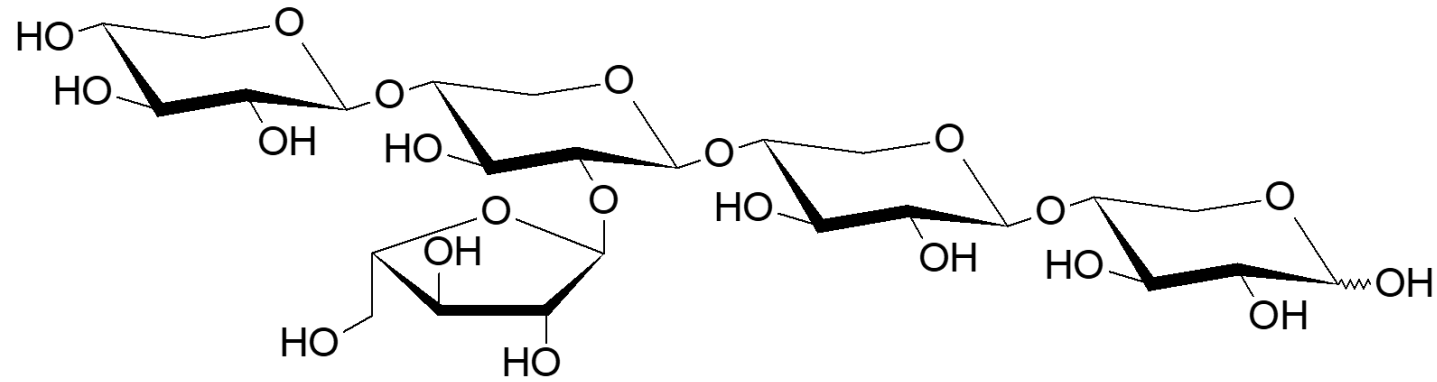

2^3-α-L-Arabinofuranosyl-xylotetraose (**XA^{2}XX**)

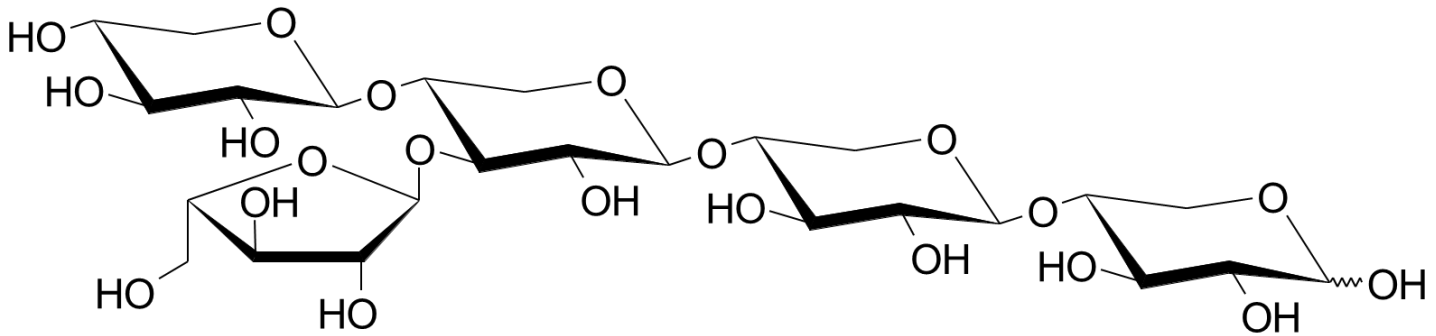

3^3-α-L-Arabinofuranosyl-xylotetraose (**XA^{3}XX**)

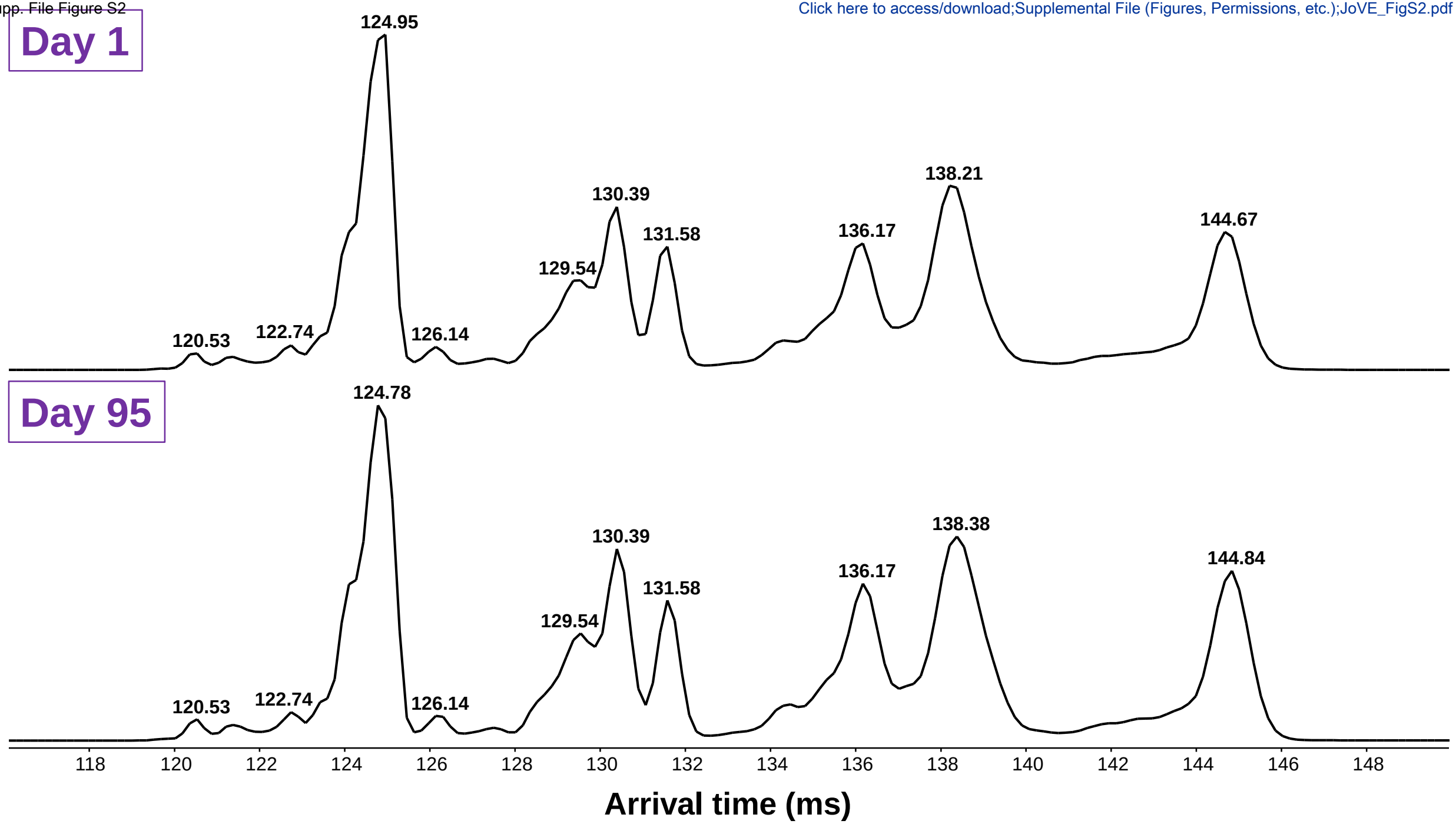

Module	Parameters
Raw data methods >Mass detection	MS level: 2 Mass detector: Wavelet transform >Noise level: 5.0E1 >Scale level: 1 >Wavelet window size: 100 %
Raw data methods >Feature detection >ADAP Chromatogram builder	MS level: 2 Min group size in # of scans: 5 Group intensity threshold: 5.0E1 Min highest intensity: 5.0E1 m/z tolerance: 0.2 m/z
Feature list methods >Feature detection >Chromatogram deconvolution	Algorithm: Wavelets (ADAP) >S/N threshold: 1 >S/N estimator: Intensity window SN >min feature height: 10 >coefficient/area threshold: 0.5 >Peak duration range: 0.00 – 100.00 >RT wavelet range: 0.00 – 0.50 m/z center calculation: MEDIAN
Feature list methods >Isotopes >Isotopic peaks grouper	m/z tolerance: 0.015 m/z Retention time tolerance: 0.5 absolute (min) Maximum charge: 5 Representative isotope: Most intense
Feature list methods >Export/Import >Export to CSV file	Field separator: “,” Export common elements: >Export row m/z >Export row retention time Export data file elements: >Peak height >Peak charge

Parameter	Previous work	This work
ESI capillary voltage	3.0 kV	2.7 kV
Cone voltage	60 V	80 V
Source offset	10 V	20 V
Desolvation temperature	300 °C	350 °C
Cone gas	0 L/h	20 L/h
Fragmentation energy[1]	190 V → 175 V → –10 V	195 V → 180 V → –10 V

[1] Given as “pre-array gradient” → “pre-array bias” → “array offset” voltage gradient

[2] Previous work: Ollivier et al. *Analytical Chemistr* y. **93** (31), 10871-10878 (2021).

Supplemental Table S3

Click here to access/download;Supplemental File (Figures, Permissions, etc.);Table S3.xlsx

m/z	Arrival time (ms)	Reference $^{DT}CCS_{N2}$ (Å²)	Calculated $^{TW}CCS_{N2}$ (Å²)	Difference (Å²)
152.0712	14.79	130.4	134.19	3.79
195.0882	16.06	138.2	140.10	1.90
215.0603	17.34	146.8	147.39	0.59
311.0814	21.16	168.4	167.62	-0.78
380.2185	25.24	191.7	189.48	-2.22
472.3216	32.13	228.7	224.90	-3.80
516.2782	28.30	211.0	204.28	-6.72
556.2771	32.64	229.8	226.55	-3.25
587.3153	31.87	228.0	222.31	-5.69
609.2812	37.48	252.3	250.38	-1.92
658.3524	34.93	243.0	237.28	-5.72
729.3895	37.99	256.0	251.95	-4.05
800.4266	41.31	271.0	267.58	-3.42
871.4637	44.62	282.0	282.86	0.86
942.5008	48.19	294.0	299.04	5.04
1013.5379	51.51	306.0	313.79	7.79
1084.5751	55.08	321.5	329.41	7.91
1155.6122	58.65	333.6	344.78	11.18
1022.0040	40.03	263.1	260.45	-2.65
1121.9976	43.60	276.5	277.07	0.57
			Mean difference (%)	
			Mean absolute difference (%)	

Difference (%)
2.91
1.38
0.40
-0.46
-1.16
-1.66
-3.18
-1.41
-2.50
-0.76
-2.35
-1.58
-1.26
0.30
1.71
2.55
2.46
3.35
-1.01
0.21
-0.10
1.63